Short-Range FMCW Radar Platform for Millimetric Displacements Measurement

Andrei Anghel, Gabriel Vasile, Remus Cacoveanu, Cornel Ioana, Silviu Ciochina

SHORT-RANGE FMCW RADAR PLATFORM FOR MILLIMETRIC DISPLACEMENTS MEASUREMENT

Andrei Anghel[⋆†] *Gabriel Vasile*[†] *Remus Cacoveanu*[⋆] *Cornel Ioana*[†] *Silviu Ciochina*[⋆]

[⋆] University POLITEHNICA of Bucharest
Faculty of Electronics, Telecommunications and Information Technology
1-3 Iuliu Maniu, Bucharest, ROMANIA
[†] CNRS / Grenoble INP, Grenoble-Image-sPeach-Signal-Automatics Lab,
38402 Grenoble Cedex, FRANCE

ABSTRACT

A frequency modulated continuous wave (FMCW) radar platform for millimetric displacement measurements of short-range targets is presented in this paper. The platform's transceiver is based on a heterodyne architecture because the beat frequency is relatively small for short-range targets and it can be placed in the frequency range influenced by the specific homodyne architecture problems: DC offset, self-mixing and 1/f noise. The platform's displacement measurement capability was tested on range profiles and SAR images acquired for various targets. The displacements were computed from the interferometric phase. The displacements errors were situated below 0.1 mm for metallic bar targets placed at a few meters from the radar.

Index Terms— Frequency Modulated Continuous Wave (FMCW), Interferometry.

1. INTRODUCTION

The frequency modulated continuous wave (FMCW) radar is an alternative to the pulse radar when the target range can be relatively small (below 100 m). In order to measure such distances with the pulse radar the switching time between transmission and reception should be at most tens of nanoseconds and the sampling frequency could reach more than 1 GHz. For a FMCW radar the range information is provided by beat frequencies and each frequency corresponds to a target placed at a certain distance. Typical FMCW radar implementations have a homodyne architecture based transceiver [1, 2] which limits the performances for short-range applications. In the case of targets positioned near the radar the beat frequency is small and can be in the band affected by the classical problems of the homodyne architecture (DC offset, self-mixing and 1/f noise) [3]. Another problem of the FMCW transceiver is that the voltage controlled oscillator (VCO) adds a certain degree of nonlinearity which leads to a deteriorated resolution by spreading the target energy through different frequencies [5]. This problem is usually solved either by hardware [4, 5, 6] or software [7, 8, 9] approaches. In this paper is presented FMCW radar platform based on a heterodyne architecture of the transceiver. The heterodyne architecture eliminates the low frequency self-mixing spectrum and reduces the noise bandwidth for better sensitivity. The nonlinearity correction algorithm used on the acquired beat signals is presented in [10]. The radar platform is tested with a number of range profiles and SAR images. The displacements are computed from the interferometric phase. The absolute error was below 0.1 mm in all tests.

The rest of this paper is organized as follows. Section 2 makes a description of the FMCW platform. In Section 3 the experimental results are presented and the conclusions are stated in Section 4.

2. FMCW PLATFORM DESCRIPTION

The block diagram of the 8-12 GHz short range FMCW radar platform is shown in Fig. 1. The command signal is a linear tuning voltage with 100 ms period obtained from the signal generator of an USB oscilloscope. The RF VCO block is a low-cost X-band VCO with 15% linearity (according to the linearity definition given in [11]) which provides the local oscillator (LO) signal. In [12] is mentioned that the slope of the frequency-voltage characteristic for some VCOs may be reasonably approximated by a quadratic curve. However, a more general approach is to assume a polynomial frequency-voltage dependence. With this assumption, for a linear tuning voltage, the RF VCO signal in a sweep period T_p can be written as:

$$s_{LO}(t) = cos\left[2\pi\left(f_0 t + \frac{1}{2}\alpha_0 t^2\right) + \Phi_{nl}(t)\right], \quad (1)$$

where

The authors would like to thank the Électricité de France (EDF) company for supporting the development of the FMCW experimental platform.

$$\Phi_{nl}(t) = \sum_{k=2}^{K} \frac{\beta_k}{k+1} t^{k+1}, \tag{2}$$

is the nonlinearity phase term (which depends on the nonlinearity coefficients β_k with $k = \overline{2, K}$), f_0 and α_0 are respectively the frequency and the linear chirp rate in the origin. The intermediary frequency (IF) block is a direct digital synthesizer with adjustable frequency (25-250kHz). The transmitted signal consists of two different signals obtained by mixing the LO signal with the IF signal:

$$s_T(t) = \frac{1}{2}\cos\left[2\pi\left((f_0 + f_{IF})t + \frac{1}{2}\alpha_0 t^2\right) + \Phi_{nl}(t)\right] + \frac{1}{2}\cos\left[2\pi\left((f_0 - f_{IF})t + \frac{1}{2}\alpha_0 t^2\right) + \Phi_{nl}(t)\right]. \tag{3}$$

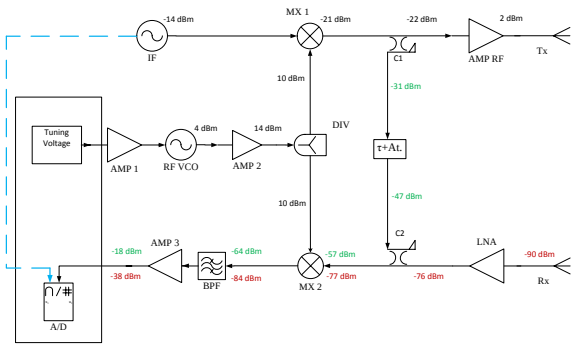

Fig. 1. Block diagram of the X-band FMCW radar platform.

A part of the transmitted signal gets directly to the receiver section mixer through the couplers (C1 and C2) and the delay line. This reference path is used as power level reference and for calibrating the radar using software nonlinearity estimation and correction solutions. In the receiver section, the reflected signal that comes from N different targets is a sum of delayed and attenuated versions of the transmitted signal $s_T(t)$:

$$s_R(t) = \sum_{i=1}^{N} A_i s_T(t - \tau_i), \tag{4}$$

where τ_i and A_i are the propagation delay and amplitude corresponding to target i. The received signal is mixed with the LO and the resulting signal gets centered around the IF:

$$s_{IF}(t) = \frac{1}{4}\sum_{i=1}^{N} A_i \Big\{ \cos\Big[2\pi\Big((f_{IF} + \alpha_0\tau_i)t + (f_0 - f_{IF})\tau_i + \frac{1}{2}\alpha_0\tau_i^2\Big) + \Phi_{nl}(t) - \Phi_{nl}(t-\tau_i)\Big] + \cos\Big[2\pi\Big((f_{IF} - \alpha_0\tau_i)t - (f_0 + f_{IF})\tau_i + \frac{1}{2}\alpha_0\tau_i^2\Big) + \Phi_{nl}(t) - \Phi_{nl}(t-\tau_i)\Big]\Big\} \tag{5}$$

For short-range applications the delay is very small compared to the sweep period. In consequence the residual video phase (RVP) term [13] can be neglected and the nonlinearity phase term difference can be approximated with the derivative multiplied with the delay. Under these assumptions, the IF signal can be rewritten as:

$$s_{IF}(t) \approx \frac{1}{4}\sum_{i=1}^{N} A_i \Big\{ \cos\Big[2\pi\Big((f_{IF} + \alpha_0\tau_i)t + (f_0 - f_{IF})\tau_i + \tau_i\sum_{k=2}^{K}\beta_k t^k\Big)\Big] + \cos\Big[2\pi\Big((f_{IF} - \alpha_0\tau_i)t - (f_0 + f_{IF})\tau_i + \tau_i\sum_{k=2}^{K}\beta_k t^k\Big)\Big]\Big\}. \tag{6}$$

This signal is filtered, amplified and afterwards is sampled with 1 MHz sample rate. The sampled signal consists of two groups of spectral components placed symmetrically around the intermediary frequency as presented in Fig. 2. The analog band-pass filter (BPF: 25-500 kHz bandwidth) removes the low-frequency components (resulted from self-mixing and local oscillator leakage in the transmitted signal) and improves the signal to noise ratio by reducing the thermal noise bandwidth. Additional digital filters can be applied to select an imposed range interval before mixing to baseband. The IF is adjusted according to the sampling frequency and the expected beat frequencies.

In order to shift the spectrum in the baseband the signal in (6) should be digitally multiplied with the sampled IF sine signal. The resulting beat frequency signal is (neglecting the 0.5 factors resulted from cosine multiplying):

$$s_b(t) = \sum_{i=1}^{N} A_i \cos\left[2\pi\left(f_0 + \alpha_0 t + \sum_{k=2}^{K}\beta_k t^k\right)\tau_i\right]. \tag{7}$$

If the range profile is computed as the Fourier transform of this signal, the nonlinearity terms spread the energy of each target and the resolution gets deteriorated. The nonlinearity correction procedure applied to the beat signal is described

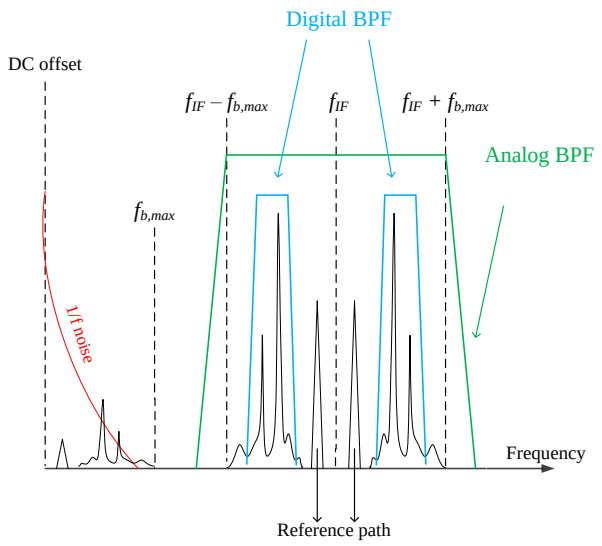

Fig. 2. Intermediary frequency signal spectrum. The analog filter removes the low-frequency components and improves the signal to noise ratio. Digital filters can be used to select a certain range interval.

in detail in [10] and can be summarized as follows. The analytical version of (7) is a sum of polynomial-phase signals whose coefficients are estimated using the high-order ambiguity function (HAF) [14] on the response obtained from the reference path. Onwards, with the estimated coefficients (α_0 and β_k) a nonlinearity correction function is built and applied through a time resampling of the beat signal. After the nonlinearity correction, the complex beat signal is expressed as:

$$s_{b,c}(t) = \sum_{i=1}^{N} A_i \exp\left[j2\pi\left(f_0\tau_i + \alpha\tau_i t\right)\right]. \qquad (8)$$

where α is the mean chirp rate defined as the ratio between bandwidth and sweep period. Notice that the corrected signal is a sum of N complex sinusoids which means that each target should appear as a *sinc* function in the range profile and the range resolution can reach the theoretical limit.

3. DISPLACEMENT MEASUREMENT RESULTS

Displacement measurements with the FMCW platform were made using both range profiles and synthetic aperture images.

3.1. Range profiles displacements

Different targets such as metallic bars and corner reflectors were placed in front of the radar at various ranges ($1 - 6m$). The target was moved with a few millimetres in successive acquisitions and the displacements were evaluated using the interferometric phase of the FMCW complex range profile. The measured displacements and absolute errors are summarized in Fig. 3.

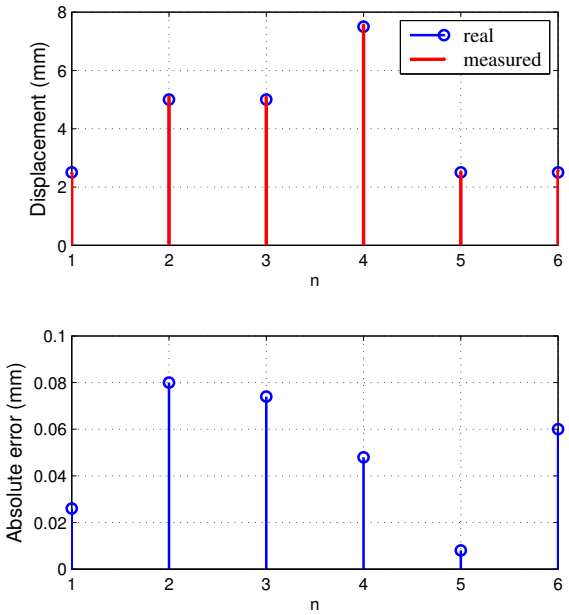

Fig. 3. Range profile displacements measurement results.

3.2. SAR Images displacements

A scene containing two metallic bars was considered. The frequency sweep interval was $9 - 10GHz$. The SAR images were obtained by moving the platform on a linear $30cm$ rail. A synthesized image is shown in Fig. 4. One of the targets was moved on different directions between image acquisitions and the displacement was projected on the local line of sight (LOS) direction. Due to the short-range the projection angle is different for the two targets. The LOS displacements were computed from the phase difference of the target pixels of two complex images. Fig. 5 shows a few measured LOS displacements and the corresponding absolute errors.

4. CONCLUSIONS

This paper has presented a FMCW radar platform used for displacement measurements of short-range targets. The platform's transceiver is based on an intermediary frequency architecture in order to avoid the specific homodyne problems and enhance the system's sensitivity. The platform's measurement capabilities were validated on range profiles and SAR images acquired for various targets. The displacements errors were situated below 0.1 mm for targets placed at a few meters from the radar.

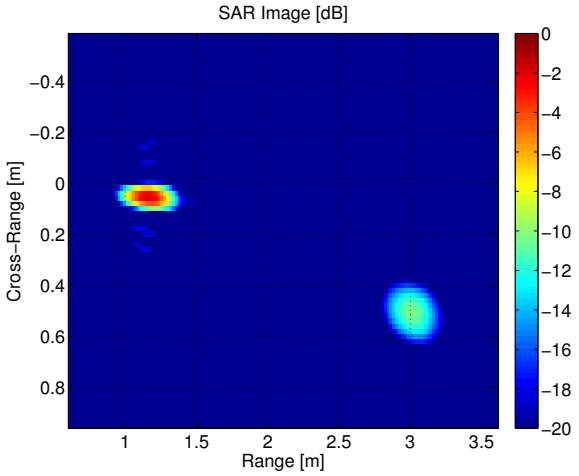

Fig. 4. SAR Image obtained for two metallic bars. The phase difference of the target pixels in different images leads to the line of sight displacement.

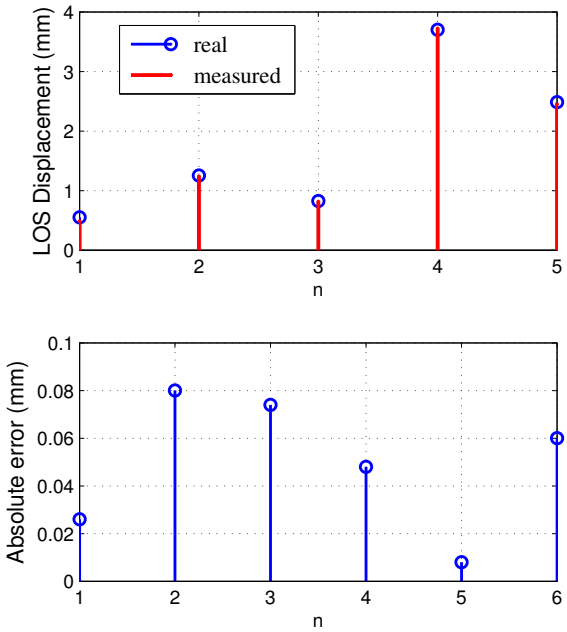

Fig. 5. SAR line of sight displacements measurement results.

5. REFERENCES

[1] A. Meta, P. Hakkart, F.V. der Zwan, P. Hoogeboom, and L. Ligthart, "First demonstration of an x-band airborne FMCW SAR," in *Proc. EuSAR'06*, Dresden, Germany, May 2006, pp. 1–4.

[2] G. L. Charvat, "Low-cost, high resolution X-band laboratory radar system for synthetic aperture radar applications," in *Proc. IEEE International Conference on Electro/information Technology*, East Lansing, MI, USA, May 2006, pp. 529–531.

[3] L. Besser and R. Gilmore, *Practical RF Circuit Design for Modern Wireless Systems*, Artech House, London, 2003.

[4] Li Li, J. Yu, and J. Krolik, "Software-defined calibration for FMCW phased-array radar," in *Proc. IEEE Radar Conference*, Washington DC, USA, May 2010, vol. 20, pp. 877–881.

[5] P. Lowbridge, "A low cost mm-wave cruise control system for automotive applications," *Microwave Journal*, pp. 24–36, Oct. 1993.

[6] Nils Pohl, Timo Jacschke, and Michael Vogt, "Ultra high resolution SAR imaging using an 80 ghz FMCW-Radar with 25 ghz bandwidth," in *Proc. EuSAR'12*, Nuremberg, Germany, Apr. 2012, pp. 189–192.

[7] M. Vossiek, P. Heide, M. Nalezinski, and V. Magori, "Novel FMCW radar system concept with adaptive compensation of phase errors," in *Proc. EuMC'96*, Prague, Czech Republic, Sept. 1996, vol. 1, pp. 135–138.

[8] A. Meta, P. Hoogeboom, and L. Ligthart, "Range nonlinearities correction in FMCW SAR," in *Proc. IGARSS'06*, Denver, Denver, USA, July 2006, pp. 403–406.

[9] W. Ying, L. Qingshan, G. Deyun, and Z. Guangyong, "Research on nonlinearity correction imaging algorithm of FMCW SAR," in *Proc. ICSPS'10*, Dalian, China, July 2010, vol. 1, pp. 425–429.

[10] A. Anghel, G. Vasile, R. Cacoveanu, C. Ioana, and S. Ciochina, "FMCW Transceiver Wideband Sweep Nonlinearity Software Correction," in *submitted to IEEE RadarCon2013*.

[11] United States Department of Defense, "General specification for crystal controlled oscillator. Specification MIL-PRF-55310," Columbus, OH.

[12] P.V. Brennan, Y. Huang, M.Ash, and K. Chetty, "Determination of sweep linearity requirements in FMCW radar systems based on simple voltage-controlled oscillator sources," *IEEE Trans. Aerosp. Electron. Syst.*, vol. 47, no. 3, pp. 1594–1604, July 2011.

[13] Walter G. Carrara, Ron S. Goodman, and Ronald M. Majewski, *Spotlight Synthetic Aperture Radar: Signal Processing Algorithms*, Artech House, Boston, 1995.

[14] Y. Wang and G. Zhou, "On the use of high order ambiguity functions for multicomponent polynomial phase signals," *Signal Processing*, vol. 65, pp. 283–296, 1998.